


Out-of-phase solitons in multicore fibers of one-dimensional and square lattices of weakly coupled cores

S. A. Skobelev,^{*} A. A. Balakin^{✉,†} and A. G. Litvak[✉]
Institute of Applied Physics RAS, 603950 Nizhny Novgorod, Russia

 (Received 17 July 2023; accepted 18 October 2023; published 7 November 2023)

Approximate solitonlike out-of-phase spatiotemporal solutions for the wave field envelope in multicore fibers with weakly coupled cores in configurations of a one-dimensional $1 \times N$ lattice and a square $N \times N$ lattice are found. The stability of these distributions for pulse durations greater than the critical duration is shown analytically and numerically. Numerical simulation of initially shorter pulses shows that the emission of linear dispersive waves rather quickly transforms them to the found solution with a duration about the critical one.

DOI: [10.1103/PhysRevA.108.053503](https://doi.org/10.1103/PhysRevA.108.053503)

I. INTRODUCTION

The concept of optical solitons—stable, localized structures formed as a result of competition between dispersion and nonlinearity—is one of the most striking effects in nonlinear optics. The great interest shown in soliton solutions of nonlinear equations is due to the fact that they play a fundamental role in the dynamics of a laser pulse in a medium. The theory of optical solitons has found application in numerous practical problems [1].

One of the disadvantages of optical solitons is that the energy of the nonlinear structure in a single fiber is inversely proportional to the pulse duration. A possible method for increasing the total energy of soliton laser pulses at a fixed duration is to switch to multichannel laser systems based on weakly coupled multicore waveguides. In this case, the total energy of a given nonlinear structure can significantly exceed the energy of a soliton of the nonlinear Schrodinger equation (NSE) in a single core. The existence of these nonlinear solutions will make it possible to generalize the well-known methods of laser pulse compression in a single fiber as applied to multicore fibers (MCFs).

A number of interesting results have been obtained for the in-phase wave distributions in MCFs: the generation of a supercontinuum [2–5], compression of laser pulses [4–10], formation of light bullets [4–7,9–12], and control of the wave field structure [13,14]. Unfortunately, there is its own critical power (energy for pulse problem), at which threshold instability of the self-focusing and self-trapping of the quasi-homogeneous distribution of the discrete wave field occurs [15]. It should be noted that the presence of its own critical power leads to the fact that the total power of the coherent laser radiation is again limited to a level that does not exceed the maximum achievable in a single-channel system.

Rather promising results were obtained in the case of using out-of-phase distributions of the wave field (the field in

neighboring cores changes sign). Stable out-of-phase distributions were found for different core configurations in MCFs: on a ring [16,17], and in the form of a one-dimensional lattice [18] and a square lattice [19]. This made it possible to propose a fundamentally different method for transporting coherent laser radiation with a power significantly exceeding the critical power of self-focusing in media. Thus, the threshold, which fundamentally limits the power in one core and free space, can be overcome, and the way to create significantly more (10 times or more) powerful coherent laser pulses in fiber optics, in comparison with currently existing ones, can be found. These studies have motivated interest in the search for stable spatiotemporal soliton solutions. The out-of-phase space-time soliton was found in an MCF consisting of an even number of cores on the ring, and a stability analysis was carried out [20]. The stable out-of-phase space-time soliton solutions were found in MCFs of 24 densely packed cores [21].

In this paper, we generalize the solitonlike solution to the case of MCFs with one-dimensional and square core lattices. Previously, stable out-of-phase steady-state solutions were found for intense wave beams in such MCFs [18,19]. At low powers, the wave field in these solutions is distributed along the sine, as in a linear rectangular waveguide. As the power increases, the wave field amplitudes in different cores become equal. The generalization of these solutions to the case of spatiotemporal solitonlike solutions is most simply performed within the framework of the variational approach, which will be tested on already known solutions. The search and analysis of the stability of new classes of stable out-of-phase solitonlike wave field distributions in MCFs from one-dimensional (Sec. III) and two-dimensional (Sec. IV) lattices of cores will be performed. Numerical simulation of the original equation will be used to demonstrate the stability of the found solutions.

II. BASE EQUATIONS

Lets consider the self-action of laser pulses in a multicore fiber, which is a rectangular lattice ($N \times M$) of weakly

^{*}sksa1981@gmail.com

[†]balakin@ipfran.ru

coupled cores. We use the weak-coupling approximation of fundamental modes guided by the cores of an optical fiber oriented parallel to the z axis [1,22]. In this case, the wave field in the MCF can be approximately represented as the sum

$$\mathcal{E}(z, t, x, y) \approx \sum_{n,m} \mathcal{E}_{n,m}(z, t) \phi(x - x_n, y - y_m), \quad (1)$$

where x_n, y_m are the coordinates of the center of the $\{n, m\}$ -th core, $\phi(x, y)$ is the structure of the fundamental mode in the core, and $\mathcal{E}_{n,m}$ is the complex amplitude of the electric field strength in the $\{n, m\}$ -th core. The summation is performed over all fiber cores.

The evolution of the wave field envelope during propagation along the z axis can be affected by linear dispersion, inertial Kerr-type nonlinearity, and interaction with the nearest-neighbor cores due to the weak overlap of fundamental modes guided by them. Assuming weak coupling between the cores that does not perturb the structure of the fundamental mode, we obtain the following system of equations for the envelope of the electric field strength $\mathcal{E}_{n,m}$ in the $\{n, m\}$ -th core [4,6]:

$$i \frac{\partial \mathcal{E}_{n,m}}{\partial z} + i \beta_1 \frac{\partial \mathcal{E}_{n,m}}{\partial t} - \frac{\beta_2}{2} \frac{\partial^2 \mathcal{E}_{n,m}}{\partial t^2} + \gamma |\mathcal{E}_{n,m}|^2 \mathcal{E}_{n,m} + \chi (\mathcal{E}_{n-1,m} + \mathcal{E}_{n+1,m} + \mathcal{E}_{n,m-1} + \mathcal{E}_{n,m+1}) = 0, \quad (2)$$

where $\beta_1 = \partial k / \partial \omega$ and $\beta_2 = \partial^2 k / \partial \omega^2$ are the first- and second-order linear dispersion coefficients for the core dispersion law $k(\omega)$, γ is the nonlinearity coefficient, and χ is the linear coupling coefficient between adjacent cores. Here we consider the case when all the cores are the same, i.e., the coefficients of linear dispersion, nonlinearity, and coupling are assumed to be the same. We will also assume that the central frequency of the laser pulse injected into the MCF lies in the region of anomalous group velocity dispersion ($\beta_2 < 0$). Equation (2) must be supplemented with boundary conditions,

$$\mathcal{E}_{n,0} = \mathcal{E}_{n,M+1} = \mathcal{E}_{0,m} = \mathcal{E}_{N+1,m} = 0. \quad (3)$$

Here we have specially added “virtual” points $n = 0, N + 1$ and $m = 0, N + 1$ at the boundaries, which corresponds to the absence of these cores in a real fiber.

In the accompanying coordinate system moving with the group velocity of the wave packet ($\tau = t - \beta_1 z$), Eqs. (2) can be written in dimensionless variables in the following form:

$$i \frac{\partial u_{n,m}}{\partial z} + \alpha \frac{\partial^2 u_{n,m}}{\partial \tau^2} + |u_{n,m}|^2 u_{n,m} + u_{n-1,m} + u_{n+1,m} + u_{n,m-1} + u_{n,m+1} = 0, \quad (4)$$

where $\alpha = -\beta_2 / (2\chi)$, $\mathcal{E}_{n,m} = u_{n,m} \sqrt{\chi/\gamma}$, $z \rightarrow z/\chi$.

Equation (4) is limited to the approximation (1) of the single-mode propagation of the wave field in each core. This approximation is violated for radiation power values in some core $\mathcal{P}_{n,m} = |\mathcal{E}_{n,m}|^2 \iint \phi^2 dx dy$, close to the critical power of self-focusing in a homogeneous medium \mathcal{P}_{cr} .

A class of stable out-of-phase soliton solutions was found [20] in a MCF consisting of an even number of cores located on a ring. This corresponds to $M = 1$ and periodic boundary conditions $u_0 = u_N$, when a supermode $u_n = (-1)^n A_{\pm}$ with the same wave field amplitude in all cores exists [16]. Here,

the term “supermode” denotes a stationary solution to a discrete problem. This made it possible to look for a solution in the class of factorized functions $u_n(z, \tau) = (-1)^n u_{\pm}(z, \tau)$, where the transverse distribution of the wave field is determined by this supermode.

Unfortunately, the ring configuration of the MCF has a number of disadvantages that may limit its practical application. First, the complexity of manufacturing such a fiber increases with N due to the requirement for a fairly accurate uniform arrangement of the cores around the ring. Second, the presence of a large unused space in the center of a multicore fiber with a large number of cores makes the transverse dimensions of the fiber large, which is not always convenient in practice.

In this paper, we consider alternative configurations of a multicore fiber, in which the cores are located along a line ($M = 1$) or on a square lattice ($M = N$). We investigate the possibility of the existence and stability of out-of-phase spatiotemporal solitary solutions in such fibers, which are localized laser pulses propagating without distortion in all available cores. We demonstrate analytically and numerically that such solutions exist for both one-dimensional and two-dimensional lattices of cores, and determine the range of parameters for the stability of the found solutions.

Unfortunately, it is quite difficult to find analytical solitary solutions for Eq. (4). A possible simplification would be to move to a smooth transverse envelope in MCF consisting of a large but finite number of cores. For example, in the case of a fiber with a rectangular core matrix $N \times M$ ($N, M \gg 1$), we will look for a solution of Eq. (4) in the form of an out-of-phase distribution $u_{n,m} = (-1)^{n+m} U(n, m, z, \tau) e^{-2iz}$. Assuming the field envelope to be a smooth function ($\frac{\partial U}{\partial n} \ll \pi U$, $\frac{\partial U}{\partial m} \ll \pi U$), we arrive at the equation of NSE type,

$$i \frac{\partial U}{\partial z} - \frac{\partial^2 U}{\partial n^2} - \frac{\partial^2 U}{\partial m^2} + |U|^2 U + \alpha \frac{\partial^2 U}{\partial \tau^2} = 0. \quad (5)$$

The sign of the nonlinearity remained the same (i.e., focusing) in the equation, but the sign of the diffraction terms changed since the out-of-phase distribution is at the edge of the Brillouin zone. As a result, the character of Eq. (5) became *defocusing* at $\alpha = 0$. This has a physical meaning of “pushing” the field in neighboring cores due to a difference in signs. In the case of a line of cores ($M = 1, N \gg 1$), we get a similar equation, but without derivatives with respect to the second index m , i.e., $\frac{\partial U}{\partial m} = 0$. Note that Eq. (5) remains Hamiltonian and its action is

$$S = \iiint \left[\frac{U \partial_z U^* - U^* \partial_z U}{2i} - \alpha \left| \frac{\partial U}{\partial \tau} \right|^2 + \left| \frac{\partial U}{\partial n} \right|^2 + \left| \frac{\partial U}{\partial m} \right|^2 + \frac{|U|^4}{2} \right] dz d\tau dn dm. \quad (6)$$

Equation (5) should be supplemented with boundary conditions corresponding to (3): $U(n, 0) = U(n, M + 1) = U(0, m) = U(N + 1, m) = 0$. Moreover, the presence of such boundary conditions qualitatively changes the nonlinear dynamics in comparison with the case of boundless media, when a kind of the wave-breaking, the dispersion-induced chirping, or the Kerr-induced phase modulation can happen. The

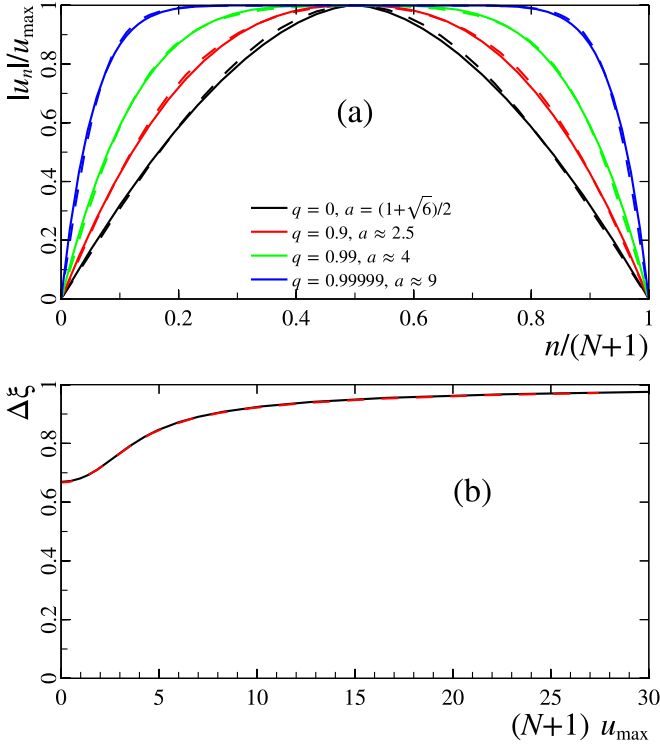


FIG. 1. (a) Structure of solutions for different parameter values. Dashed line: exact solution U_{\pm} (7); solid line: power-law distribution of the wave field U_{beam} (9). (b) Dependence of the width of $\Delta\xi$ (14), (15) on the maximum amplitude u_{max} in exact (dashed) and approximate (solid) solutions.

presence of boundary conditions makes the problem similar to waveguide propagation, in which the fundamental mode (a continuous analog of the supermode) is unique and stable. For example, a solution similar to parabolic pulses [23] in boundless media will correspond to the initial dynamics of a very narrow wave field, containing a lot of waveguide modes, in the area far from waveguide boundaries. Contrary, single-mode solutions are of interest in this paper due to their robustness and predictability.

III. ONE-DIMENSIONAL LATTICE

Consider first the case of cores located along the line. In the case of beams ($\alpha = 0$), a stable out-of-phase supermode is found [18], using the Jacobi sine,

$$U_{\pm} = U_0 \text{sn}(\varkappa n, q) e^{-i\lambda z}, \quad 2q\varkappa^2 = U_0^2, \\ (N + 1)\varkappa = 2K(q), \quad \lambda = (1 + q)\varkappa^2. \quad (7)$$

Here, $K(q) = \int_0^{\pi/2} \frac{d\psi}{\sqrt{1-q\sin^2\psi}}$ is the complete elliptic integral of the first kind, and the parameter q varies in the range $[0, 1)$ and is found from the transcendental equation

$$qK(q)^2 = \frac{1}{8}(N + 1)^2 U_0^2. \quad (8)$$

The structure of the found out-of-phase supermode (7) for different values of the parameter q is shown by a dotted line in Fig. 1(a). Here, the field distribution is normalized to the maximum value.

The intensity distribution of the supermode is nonuniform in the transverse direction [Fig. 1(a)] and is well approximated by the dependence $|U_{\pm}|^2 \propto \sin^2 \frac{\pi n}{N+1}$ in the case of low power, while at high power the field intensity is uniformly distributed over all cores, $|U_{\pm}|^2 \propto \text{const}$. The solution (7) is similar in form to cnoidal waves, but was obtained for Eq. (5) with defocusing nonlinearity. Therefore, it gives a smoothing of the maxima instead of their highlighting, as in cnoidal waves.

Unfortunately, the authors are not aware of a generalization of solution (7) in the simplest special functions to the multi-dimensional case (rectangular lattice of cores) and to the case of pulses ($\alpha \neq 0$). Therefore, to construct a *approximate* out-of-phase space-time soliton solution, we use the variational approach.

A. Beam problem ($\alpha = 0$)

To test the variational approach, we consider the MCF configuration of an MCF with known solution (7) for the wave field and obtain its approximate analog. Good agreement with the solution (7) can be obtained for the power-law distribution on the transverse coordinate,

$$U_{\text{beam}} = \sqrt{\frac{P(a+1)(2a+1)}{2(N+1)a^2}} (1 - |\xi|^a) e^{ib|\xi|^a + i\varphi}, \quad (9)$$

where $\xi = \frac{2n}{N+1} - 1$, $P = \frac{2}{N+1} \int_{-1}^1 |U_{\text{beam}}|^2 d\xi \approx \sum |u_n|^2$ is the wave field power, which is preserved in the process of evolution. We took into account that the inhomogeneous phase shift across the beam is proportional to the inhomogeneity of its amplitude ($\propto b|\xi|^a$). The power-law distribution (9) describes the exact solution for the supermode (7) quite well over a wide range of parameters q, a [Fig. 1(a)]. It should be noted that the limiting case of the linear problem [$q = 0$ in the solution (7)] corresponds to the power-law distribution (9) at

$$a_{\text{min}} = (1 + \sqrt{6})/2 \approx 1.72. \quad (10)$$

Substituting expression (9) into the action (6) of Eq. (5) with $\alpha = 0$, we find the truncated action

$$S = \int \frac{P}{N+1} \left[\frac{3P}{N+1} \frac{(a+1)(2a+1)}{(3a+1)(4a+1)} + \frac{(4a^2b^2 + 24a^2 - 14a + 2)(a+1)(2a+1)}{(2a-1)(3a-1)(4a-1)(N+1)^2} + \frac{d\varphi}{dz} + \frac{1}{3a+1} \frac{db}{dz} - \frac{11a^2 + 12a + 3}{(a+1)(2a+1)(3a+1)^2} b \frac{da}{dz} \right] dz. \quad (11)$$

Then the change in the parameters $\mathbf{p} = \{a, b, \varphi\}$ of the wave field [Eq. (9)] along the MCF is determined by the Euler equations

$$\frac{d}{dz} \frac{\partial \mathcal{L}}{\partial \dot{p}_j} - \frac{\partial \mathcal{L}}{\partial p_j} = 0, \quad \dot{p}_j = \frac{dp_j}{dz}, \quad (12)$$

where Eq. (11) is used as the action $S = \int \mathcal{L} dz$. The resulting equations have a stationary point (center type) at

$$P = \frac{(3a+1)^2(4a+1)^2(4a^2 - 4a - 5)}{3(N+1)(2a-1)^2(11a^2 + 10a + 2)}, \quad b = 0, \quad (13)$$

corresponding to a stable out-of-phase distribution. Note that Eq. (13) has a single real root at $a \geq a_{\min}$ for any value of P . Here, $P = 0$ is achieved at $a = a_{\min}$ and there is the asymptotic $P \approx \frac{48}{11} a^2 / (N + 1)$ at $P \rightarrow \infty$.

Let us compare the found approximate solution (9) at the stationary point (13) with the exact solution (7). Figure 1(b) shows the dependence of the wave beam width $\Delta\xi$, determined from the level of the field amplitude decreased by a factor of two, on the maximum amplitude u_{\max} . For the approximate solution, it is equal to

$$\Delta\xi = 1/\sqrt[3]{2}, \quad (14)$$

and for the exact solution,

$$\Delta\xi = 1 - \frac{F\left(\frac{\pi}{6}, q\right)}{K(q)} \approx 1 - \frac{\ln 3}{\ln 8 - \ln(1 - q)}, \quad (15)$$

where $F(\psi, q)$ is an incomplete elliptic integral of the second kind. Figure 1(b) shows good agreement between the exact (dashed line) and the approximate (solid line) solutions.

Additional numerical calculations were carried out within the framework of Eq. (4), which showed that the found approximate solution (13) quite well describes the wave field propagation in a one-dimensional lattice with $N \geq 5$. Thus, the approximate solution (9), (13) adequately describes the transformation of the spatial distribution of the wave field from the inhomogeneous ($|u_n|^2 \propto \sin^2[\pi n/(N + 1)]$) to a homogeneous ($|u_n|^2 \propto \text{const}$) intensity distribution with increasing power. This allows us to hope that the approximate out-of-phase space-time solitonlike solution will have the same good accuracy.

B. Pulse problem ($\alpha \neq 0$)

Next, we use the variational approximation to find an out-of-phase spatiotemporal quasisoliton solution in the framework of the two-dimensional equation (5). It is reasonable to use the class of factorized functions, where the longitudinal wave field distribution in all cores corresponds to the NSE soliton, and the transverse distribution is determined by the approximate solution (9):

$$U_{\text{sol}}^{1D} = \sqrt{\frac{W(a+1)(2a+1)}{4(N+1)a^2\tau_p}} (1 - |\xi|^a) \frac{e^{ib|\xi|^a + i\sigma\tau^2 + i\varphi}}{\cosh(\tau/\tau_p)}, \quad (16)$$

where W is the total energy, τ_p is the soliton duration, σ is the time frequency modulation parameter, and b is the phase front curvature. Here we have used the conservation of total energy, $W = \iint |U|^2 d\xi d\tau$.

Substituting distribution (16) into action (6) and integrating over the variables τ, ξ , we find the truncated action (we use the computer algebra system Wxmaxima [24] to prove it),

$$S = \int \frac{W}{N+1} \left[\frac{W}{(N+1)\tau_p} \frac{(a+1)(2a+1)}{(3a+1)(4a+1)} + \frac{(4a^2b^2 + 24a^2 - 14a + 2)(a+1)(2a+1)}{(2a-1)(3a-1)(4a-1)(N+1)^2} \right] dz, \quad (17)$$

$$+ \alpha \frac{1 + \pi^2 \sigma^2 \tau_p^4}{3\tau_p^2} - \frac{11a^2 + 12a + 3}{(a+1)(2a+1)(3a+1)^2} b \frac{da}{dz} + \frac{1}{3a+1} \frac{db}{dz} + \frac{\pi^2 \tau_p^2}{12} \frac{d\sigma}{dz} + \frac{d\varphi}{dz} \Big] dz. \quad (17)$$

The change in parameters $\mathbf{p} = \{a, b, \tau_p, \sigma, \varphi\}$ of the wave field (16) along the MCF is determined by the Euler equations (12) for the action (17). The resulting equations have a stationary point (center type) at $b = \sigma = 0$ and

$$\frac{W}{\tau_p} = \frac{(3a+1)^2(4a+1)(4a^2 - 4a - 5)}{(N+1)(2a-1)^2(11a^2 + 10a + 2)}, \quad (18a)$$

$$W = \frac{\alpha}{\tau_p} \frac{2(N+1)(3a+1)(4a+1)}{3(a+1)(2a+1)}, \quad (18b)$$

corresponding to the solitonlike propagation of the laser pulse. Oscillations near this center are similar to those in the quasisoliton duration in the framework of a one-dimensional NSE. Unfortunately, it is difficult to find a solution to Eqs. (18) for arbitrary values of the energy W . However, it is easy to find the solution asymptotics for small values of the energy W ,

$$a \approx a_{\min} + \frac{1}{200} \frac{W^2}{\alpha}, \quad a_{\min} = \frac{1 + \sqrt{6}}{2}, \quad (19a)$$

$$\tau_p \approx \frac{8}{3} \frac{(N+1)\alpha}{W} + \frac{(N+1)W}{439}. \quad (19b)$$

Here, we replace complicated root expressions by integers close to them (with a difference of less than 1%).

For a small parameter $a \approx a_{\min}$, the transverse distribution of the found solution is fairly close to sine profile $|u_n| \propto \sin(\frac{\pi n}{N+1})$, while the corresponding duration in the longitudinal direction is large and the energy increases according to the root law $W \approx \sqrt{200\alpha(a - a_{\min})}$. As the parameter a increases, the transverse distribution of the found solution transforms to a homogeneous one, the duration tends to zero, and the energy tends to infinity.

Let us study the stability of the found approximate out-of-phase soliton-like solution. The assumption of the uniformity of the longitudinal distribution of the wave field over MCF cores in solution (16) is possible only under conditions when the transverse structure is formed faster than the longitudinal one.

The out-of-phase soliton in the MCF with a ring configuration, in which field amplitudes are uniform across the cores, is stable [25] when the dispersion length $L_{\text{dis}} = \tau_p^2/\alpha$ exceeds the coupling length 2π . Since we are looking for a stationary solution in solitonlike form, the dispersion length is exactly equal to the nonlinear one. Unfortunately, the spatial distribution of the out-of-phase mode is inhomogeneous in the transverse direction and depends on the field amplitude (7) in the MCF with the line configuration of cores. The found solution (16), (18) should be expected to be stable if the dispersion length of the laser pulse exceeds the beat length between the out-of-phase and the next-nearest supermodes of the MCF,

$$\frac{\tau_p^2}{\alpha} \gg \frac{2\pi}{\Delta h}. \quad (20)$$

The linear propagation constant in the absence of dispersion in the considered MCF has the form

$$h_n = 2 \cos\left(\frac{\pi n}{N+1}\right). \quad (21)$$

The smallest of them, $h_N = 2 \cos[\pi N/(N+1)]$, corresponds to the out-of-phase distribution. Then the difference in the propagation constant between the out-of-phase and the next-nearest supermodes is

$$\Delta h = 4 \sin\left(\frac{\pi/2}{N+1}\right) \sin\left(\frac{3\pi/2}{N+1}\right) \underset{N \gg 1}{\approx} \frac{3\pi^2}{(N+1)^2}. \quad (22)$$

If, for some reason, asymmetric supermodes are forbidden, then the nearest symmetric supermode will have $h_{N-2} = 2 \cos(\pi \frac{N-2}{N-1})$ and give

$$\Delta h = 4 \sin\left(\frac{\pi}{N+1}\right) \sin\left(\frac{2\pi}{N+1}\right) \underset{N \gg 1}{\approx} \frac{8\pi^2}{(N+1)^2}. \quad (23)$$

We use the expansion (19) for obtaining the stability condition. According to Eq. (20), the found approximate solution (16) with parameters (19) will be stable in the case

$$\begin{aligned} \tau_p \gg \tau_{cr} &\equiv (N+1) \sqrt{\frac{2\alpha}{3\pi}} \quad \text{or} \\ W \ll W_{cr}^{1D} &\equiv \sqrt{\frac{32\pi\alpha}{3}}, \quad a \approx a_{min}. \end{aligned} \quad (24)$$

Thus, the transverse distribution of the found approximate solution is always close to the linear case [$|u_n|^2 \propto \sin^2(\frac{\pi n}{N+1})$] and noticeable equalization of the amplitudes over the cores does not occur, in contrast to the beam problem ($\alpha = 0$, Sec. III A). It follows from the condition (24) that the maximum admissible energy of stable solutions is bounded from above and does not depend on the number of cores. For relatively long pulses $\tau_p \gg \tau_{cr}$, the energy is approximately $N/2$ times greater than the NSE soliton energy with the same duration in a single-core fiber.

C. Numerical simulation

To demonstrate the stability of the found out-of-phase spatiotemporal solitonlike solution in a MCF with a one-dimensional lattice, let us turn to numerical simulation of the initial Eq. (4). A laser pulse was injected at the input of MCF in the form

$$\begin{aligned} u_n &= (-1)^n \sqrt{\frac{W(a+1)(2a+1)}{4(N+1)a^2\tau_p}} \frac{1 - |\xi_n|^a}{\cosh(\tau/\tau_p)}, \\ \xi_n &= 2n/(N+1) - 1, \quad n = 1 \dots N. \end{aligned} \quad (25)$$

Such pulse shape can be expanded in only odd modes ($u_n = \sum c_{2k+1} \sin \frac{\pi(2k+1)n}{N+1}$), which automatically allows only symmetric perturbations with wave numbers $h_{2k+1} = 2 \cos(\frac{\pi(2k+1)}{N+1})$, i.e., the minimum propagation index difference for perturbations is given by (23).

Let us first consider the case when the initial duration of the laser pulse exceeds the threshold value $\tau_p > \tau_{cr}$ [Eq. (24)]. Figure 2 shows the typical dynamics of a wave packet at $a = 1.8$ in an MCF consisting of $N = 11$ cores. In this case, the dispersion length is 22.5 and the beat length between adjacent

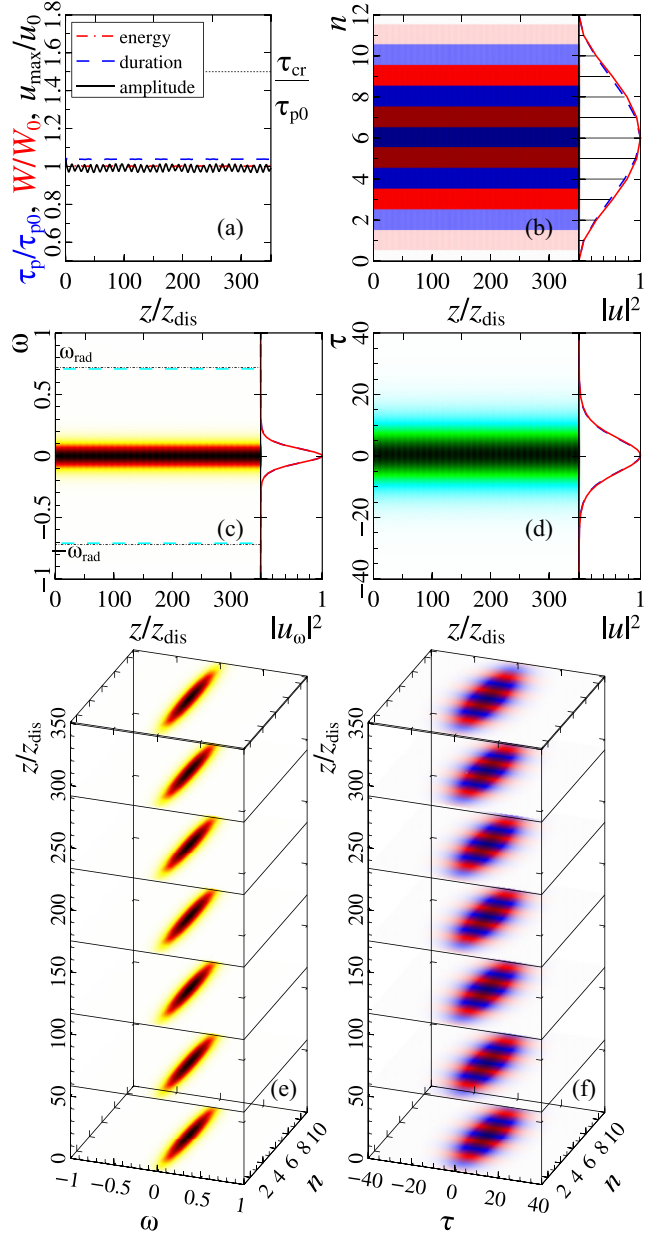


FIG. 2. Pulse dynamics in MCF of 11 cores at $a = 1.8$. (a) Dependencies of the wave-packet duration (blue dashed), energy (red dash-dotted), and maximum amplitude (black line) on the coordinate z . Evolution of the real part of the wave field over (b) cores, (c) the spectrum, and (d) the envelope in the central core along the z axis. Insets: The wave field distribution at the input (blue dashed) and at the output (red line). Slices of (e) the spectrum and (f) the envelope.

modes is 12. In Fig. 2(a), the duration τ_p , the maximum amplitude u_{max} , and the laser pulse energy W are normalized to initial values. The z coordinate is normalized to the dispersion length. Figures 2(e) and 2(f) show the two-dimensional evolution of the spectral intensity and electric field $|u_n|Re(u_n)$ along the fiber. The remaining figures show slices of the wave field in the longitudinal and transverse directions. In particular, Fig. 2(b) shows the evolution of the field dynamics $|u_n|Re(u_n)$ in the transverse direction at $\tau = 0$. This figure demonstrates the preservation of the relative phase difference between

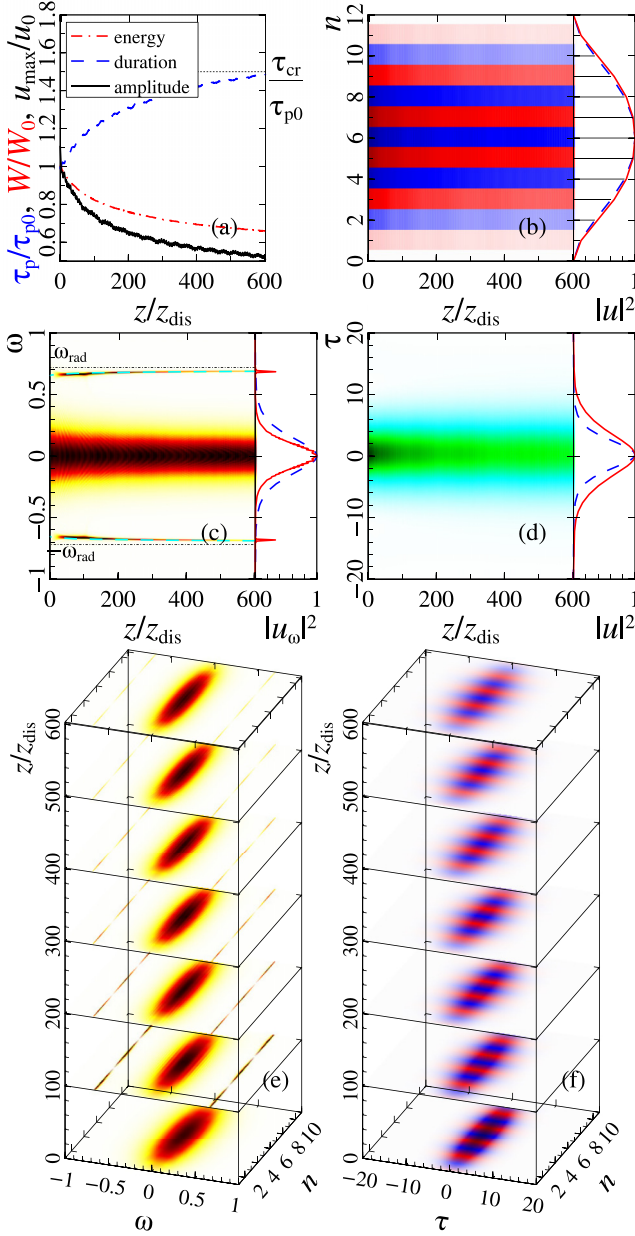


FIG. 3. Pulse dynamics in an MCF of 11 cores at $a = 2.2$. Similar to Fig. 2.

adjacent cores. Figures 2(c) and 2(d) show the evolutions of the spectrum and the field envelope $|u_n|^2$ in the central core (i.e., for $n = 6$). The insets to the right of the figures show the initial (blue dashed line) and output (red solid line) distributions. Thus, the results of numerical simulation demonstrate a stable propagation of the found out-of-phase spatiotemporal solution with keeping of its shape, total energy, and relative phase difference between adjacent cores over the calculated interval $350z_{\text{dis}}$, when the dispersion length exceeds the beat length between two adjacent modes. This confirms the stability of the found analytical solution.

Next, we numerically analyze the case when the dispersion length of the injected laser pulse is less than the beat length between adjacent supermodes ($\tau_p < \tau_{\text{cr}}$), i.e., when

the predicted stability condition of the found solution (24) is violated. Figure 3 shows the typical dynamics of a wave packet at $a = 2.2$ in an MCF consisting of $N = 11$ cores, $600z_{\text{dis}}$ long. In this case, the dispersion length is 5.7 and the beat length between neighboring modes is 12. At the initial stage $z \lesssim 150z_{\text{dis}}$, the laser pulse intensely radiates a dispersive wave at the frequency $\omega_{\text{rad}}^{\text{1D}}$, the estimate for which is given below [Eq. (31)]. The width of the laser pulse spectrum monotonically decreases and its duration, accordingly, monotonically increases as the energy in the wave packet decreases [Fig. 3(a)]. The laser pulse stops radiating when the dispersion length of the excited nonlinear structure exceeds the beat length between neighboring supermodes. Subsequently, the laser pulse propagates unchanged. Note that the group velocity of dispersive radiation differs from the group velocity of the laser pulse, which further leads to the isolation of the wave packet from the background radiation.

Let us estimate the frequency $\omega_{\text{rad}}^{\text{1D}}$ of the dispersive wave. In the case of a single-core NSE, there is a well-known stable soliton solution $u = \frac{\sqrt{2}}{\tau_p \cosh(\tau/\tau_p)}$. The NSE soliton does not interact with radiation since the wave numbers of the soliton lie in the region forbidden for linear dispersive waves. Therefore, there can be no resonance and energy exchange between the solitons and linear waves. When higher-order dispersion is taken into account, the spectrum of linear waves becomes wider and can overlap with the region of the soliton spectrum. Consequently, solitons can not only interact with radiation, but also begin to radiate linear waves. In the case of MCFs, the presence of a lattice can also make it possible to radiate dispersive waves.

Let us obtain a more simplified solution to determine the wave number of the solitary solution. The stability analysis (24) and the results of numerical simulation (Fig. 3) show that the transverse distribution of the wave packet is close to sine profile $|u_n| \propto \sin(\frac{\pi n}{N+1})$. So, we can look for a very approximate solution of Eq. (4) in the form

$$u_n = (-1)^n \sin\left(\frac{\pi n}{N+1}\right) A(z, \tau). \quad (26)$$

Substituting into the action of Eq. (4) for $M = 1$, we find the truncated action

$$S = \frac{N+1}{2} \iint \left[\frac{i}{2} \left(A \frac{\partial A^*}{\partial z} - A^* \frac{\partial A}{\partial z} \right) + 2 \cos\left(\frac{\pi}{N+1}\right) |A|^2 + \alpha \left| \frac{\partial A}{\partial \tau} \right|^2 - \frac{3}{8} |A|^4 \right]. \quad (27)$$

Its variation gives the NSE equation

$$i \frac{\partial A}{\partial z} + \alpha \frac{\partial^2 A}{\partial \tau^2} + \frac{3}{4} |A|^2 A - 2 \cos\left(\frac{\pi}{N+1}\right) A = 0, \quad (28)$$

whose soliton solution is

$$u_n = (-1)^n \sqrt{\frac{4}{3}} \frac{\sqrt{2\alpha}/\tau_p}{\cosh(\tau/\tau_p)} \sin\left(\frac{\pi n}{N+1}\right) e^{-ik_{\text{sol}}^{\text{1D}} z}. \quad (29)$$

Here, $k_{\text{sol}}^{\text{1D}} = 2 \cos(\frac{\pi}{N+1}) - \frac{3}{8} u_0^2$ is the wave number of a soliton in a one-dimensional array of weakly coupled cores and u_0 is the soliton amplitude. Note that varying the action (17) on W will give a similar value, $k_{\text{sol}}^{\text{1D}} \equiv -d\varphi/dz$. The linear

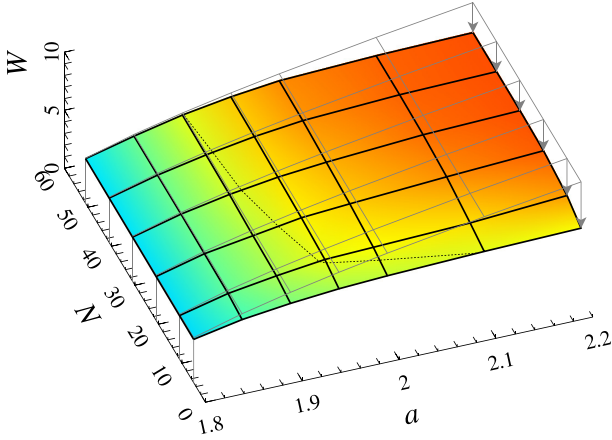


FIG. 4. Dependence of the final energy W of the excited out-of-phase soliton on the number of cores, N , and the power parameter a . The dots show the critical energy level (24).

dispersion relation of Eq. (4) at $M = 1$ looks like, for $u_n \propto (-1)^n e^{-ikz+ikn-i\omega\tau}$,

$$k_{\text{dis}}^{1\text{D}} = \alpha\omega^2 + 2 \cos \kappa_n, \quad \kappa_n = \frac{\pi n}{N+1}. \quad (30)$$

Due to the symmetry, the considered soliton can radiate a dispersive wave at the frequency ω_{rad} with odd n . Then the nearest radiated frequency is

$$\omega_{\text{rad}}^{1\text{D}} = \pm \frac{1}{\sqrt{\alpha}} \sqrt{4 \sin\left(\frac{\pi}{N+1}\right) \sin\left(\frac{2\pi}{N+1}\right) - \frac{3}{8}u_0^2}. \quad (31)$$

The cyan dashes in Fig. 3(c) show the found estimate of the dispersive wave frequency [Eq. (31)], which is in good agreement with the results of the numerical simulation. As the amplitude of the soliton decreases due to losses, the dispersive wave frequency shifts to the one determined in the limit of small amplitudes ($u_0 \approx 0$), which is shown in the figure by the black dash-dotted line.

To conclude this section, we discuss the results of numerical simulations corresponding to large values of the parameter a . As noted above, in the case of a beam problem, with increasing power, the stable spatial distribution of the wave field transforms from the inhomogeneous sine profile to a uniform distribution [18]. According to the formulas (16), (18), such a transformation should occur for the spatial distribution of the found out-of-phase solitary solution with increasing energy (increasing the parameter a). Unfortunately, in the case of a pulse problem, this does not happen due to the mechanism of generation of dispersive waves, which leads to a decrease in energy and, accordingly, to an increase in the duration of the wave packet to such values when the dispersion length exceeds the beat one. Figure 4 shows the energy of the excited nonlinear structure as a function of the number of cores, N , and the parameter a . It can be seen that the final energy is bounded from above and does not depend on the number of cores, which is in good agreement with the qualitative estimate [Eq. (24)]. The arrows in the figure show the change in energy from the initial value to the current one. It should be noted that for even larger values of $a > 5$ [which corresponds to a beam distribution close to the homogeneous one; see

Fig. 1(a)], a cascade of dispersive waves is generated at different frequencies and a faster decrease in the pulse energy up to the threshold value occurs. Thus, the change in the transverse structure of the out-of-phase spatiotemporal solitonlike solution is negligible, in contrast to the beam problem. Therefore, as a solution to Eq. (4) in the case of a one-dimensional lattice, one can use the approximate solution [Eq. (29)] at energies not higher than those given in Eq. (24).

IV. SQUARE LATTICE

In the previous section, a new class of out-of-phase solitary solutions was found in a one-dimensional lattice of cores ($M = 1$). It is shown that the maximum achievable energy of the found nonlinear structure does not depend on the number of cores, N , due to the generation of a dispersive wave. In this regard, the question arises of the existence of a stable solitary solution in a square lattice ($N \times N$) in order to be able to scale the maximum achievable energy from the number of cores. To answer this question, we use the variational approximation to find a solution in the framework of the three-dimensional NSE (5) in the class of functions

$$U_{\text{sol}}^{2\text{D}} = \sqrt{\frac{W}{\tau_p} \frac{(a+1)(2a+1)}{4(N+1)a^2}} (1 - |\xi|^a)(1 - |\zeta|^a) \times \frac{e^{ib(|\xi|^a + |\zeta|^a) + i\sigma\tau^2 + i\varphi}}{\cosh(\tau/\tau_p)}, \quad (32)$$

where $\xi = 2n/(N+1) - 1$, $\zeta = 2m/(N+1) - 1$. Substituting it into Eq. (6), we find a truncated action,

$$S = \int \frac{W}{(N+1)^2} \left[\frac{3W}{N^2\tau_p} \frac{(a+1)^2(2a+1)^2}{(3a+1)^2(4a+1)^2} + \frac{4(2a^2b^2 + 12a^2 - 7a + 1)(a+1)(2a+1)}{(2a-1)(3a-1)(4a-1)(N+1)^2} + \alpha \frac{1 + \pi^2\sigma^2\tau_p^4}{3\tau_p^2} - \frac{2(11a^2 + 12a + 3)}{(a+1)(2a+1)(3a+1)^2} b \frac{da}{dz} + \frac{2}{3a+1} \frac{db}{dz} + \frac{\pi^2\tau_p^2}{12} \frac{d\sigma}{dz} + \frac{d\varphi}{dz} \right] dz. \quad (33)$$

By varying action (33), we obtain equations for the parameters a , b , τ_p , and σ . The resulting equations have a stationary point (center type) at $b = \sigma = 0$ and

$$\frac{W}{\tau_p} = \frac{(3a+1)^3(4a+1)^3(4a^2 - 4a - 5)}{3(a+1)(2a+1)(2a-1)^2(11a^2 + 10a + 2)}, \quad (34a)$$

$$W = \frac{\alpha}{\tau_p} \frac{2(N+1)^2(3a+1)^2(4a+1)^2}{9(a+1)^2(2a+1)^2}. \quad (34b)$$

This is a system of two nonlinear equations for two unknowns a and τ_p . Solving Eq. (33) for arbitrary energies W is difficult. Again, it is easy to find the asymptotics at low energies,

$$a \approx a_{\text{min}} + \frac{1}{360} \frac{W^2}{\alpha(N+1)^2}, \quad \tau_p \approx \frac{32}{9} \frac{(N+1)^2\alpha}{W} + \frac{W}{585}. \quad (35)$$

Here complicated root expressions are replaced by integers close to them (with a difference of less than 1%).

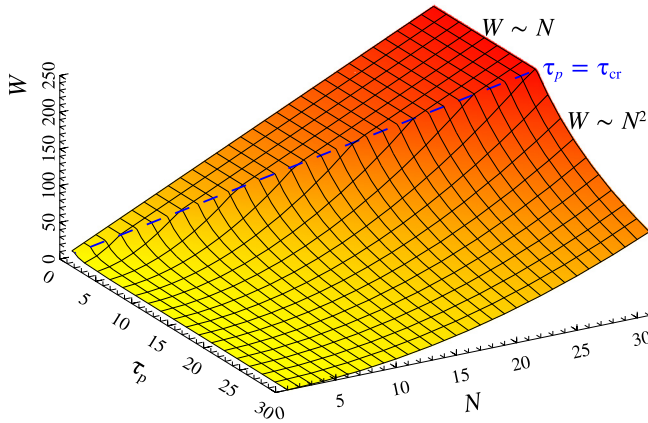


FIG. 5. Dependence of the energy W of the excited out-of-phase soliton on the number of cores, N , and the duration τ_p according to the formulas (35) and (36). The dashed line shows the level of the critical duration [Eq. (24)].

The stability of the solution [Eq. (32)] with parameters given in Eq. (34) should be expected for durations exceeding the critical value $\tau_p \gg \tau_{cr}$, as in the case of a one-dimensional lattice [Eq. (24)]. The duration limit estimate will not change. The changes will affect only the maximum achievable energy,

$$W \ll W_{cr}^{2D} \equiv \frac{16}{9} \sqrt{6\pi\alpha(N+1)}, \quad (36)$$

growing in a two-dimensional lattice proportionally to the number N , in contrast to the case of a one-dimensional lattice [Eq. (24)].

It should be noted that the condition (36) gives an increase in the *maximum achievable* energy of stable out-of-phase solitonlike distributions only in proportion to N for a fiber with $N \times N$ cores. However, the energy of the found distributions is approximately $N^2/2$ times greater than the energy of a soliton pulse of the same duration [Eq. (35)] in a single-core fiber. Therefore, for relatively long pulses $\tau_p \gg \tau_{cr}$, the gain from using fibers with a square core matrix is obvious (Fig. 5).

Let us turn to numerical simulation of the initial equation (4) to demonstrate the stability of the found out-of-phase spatiotemporal solitonlike solution in a MCF with a two-dimensional lattice of cores. A laser pulse was injected at the MCF input,

$$u_{n,m} = (-1)^{n+m} \sqrt{\frac{W}{\tau_p} \frac{2a^2 + 3a + 1}{4(N+1)a^2} \frac{(1 - |\xi_n|^a)(1 - |\zeta_m|^a)}{\cosh(\tau/\tau_p)}, \quad (37)$$

where $\xi_n = \zeta_n = 2n/(N+1) - 1$ and $n, m = 1, \dots, N$. Such a pulse shape automatically means the presence of only symmetrical perturbations, i.e., the minimum propagation constant difference for noise was given by Eq. (23).

Let us give a small explanation. A problem arises in displaying the three-dimensional wave field distribution in the case of a two-dimensional lattice. In the case of a discrete system, the renumbering of MCF cores solves this problem, i.e., efficient transition from a two-dimensional lattice to a one-dimensional one. Let us explain this using the example of a fiber with a square matrix of 11×11 cores (Fig. 6). It is

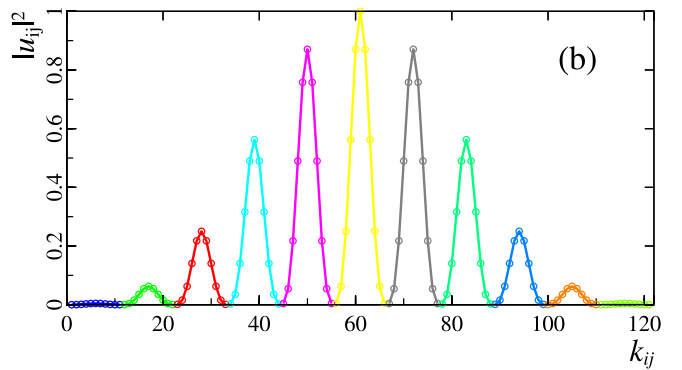
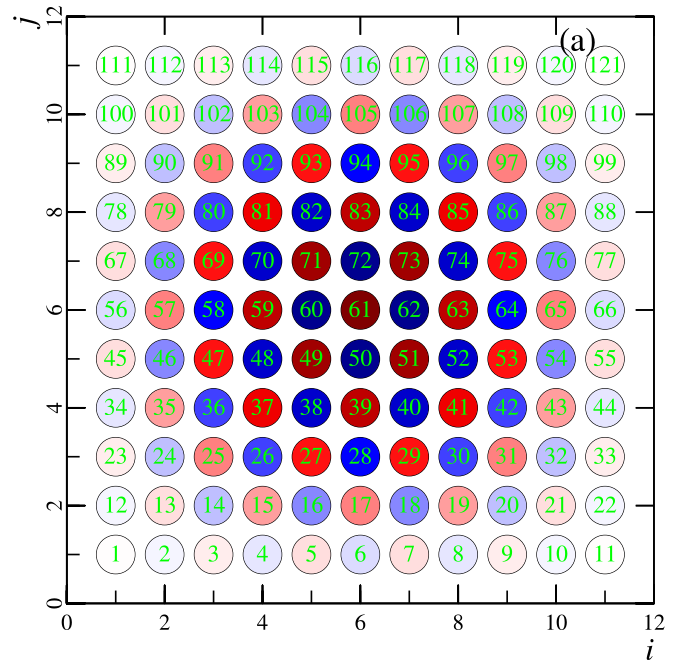


FIG. 6. (a) Example of the wave field distribution and continuous numbering of the cores in a fiber of 11 cores. (b) Normalized intensity in the cores from the continuous numbering index. Distributions in different rows are colored differently.

common to use two indices to designate the core in a rectangular matrix, for example, $u_{n,m}$ with $n, m = 1, \dots, N$. On the other hand, the same array of cores can be described by a single continuous index, $k_{n,m} = n + Nm \in 1 \dots 121$. The first representation is visual and convenient for theoretical analysis, and the last one is more convenient for numerical simulations of the wave fields' dynamics and displaying the results. Figure 6(a) shows a two-dimensional distribution of the wave field intensity of the form $|u_{n,m}|^2 = \sin^2(\frac{\pi n}{N+1}) \sin^2(\frac{\pi m}{N+1})$, and Fig. 6(b) shows the same distribution of the continuous numbering index k .

Let us return to numerical results and consider first the case of large initial pulse duration exceeding the threshold value $\tau_p > \tau_{cr}$. Figure 7 shows the typical dynamics of a wave packet at $a = 1.8$ in an MCF consisting of 11×11 cores ($N = 11$), $500z_{dis}$ in length. The continuous numbering of the cores, $k_{n,m} = n + Nm$, is used in the figure. The figure structure and captions are the same as in Fig. 2. Figures 7(c) and 7(d) show

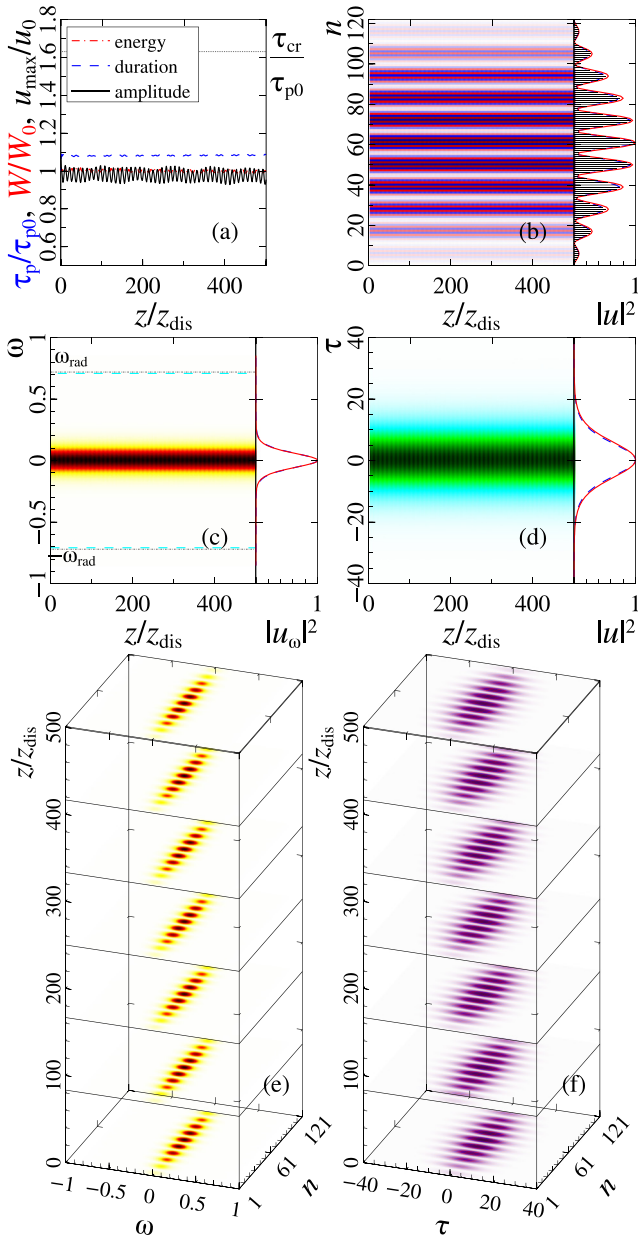


FIG. 7. Laser pulse dynamics in an MCF of 11×11 cores at $a = 1.8$. The continuous numbering of the cores, $k_{n,m} = n + Nm$, is used in the figure. Figure captions are similar to Fig. 2.

the evolution of the spectrum and the field envelope $|u_{k_{n,m}}|^2$ in the central core $n = m = 6$. It can be seen from Fig. 7 that the found solution (37) propagates without changes through the MCF over the calculated interval of $500z_{\text{dis}}$. This confirms the stability of the found analytical solution.

Next, we numerically analyze the case when the dispersion length of the injected laser pulse is less than the beat length between adjacent modes ($\tau_p < \tau_{cr}$, i.e., when the predicted stability condition of the found solution is violated). Figure 8 shows the typical dynamics of a wave packet at $a = 2.2$ in a multicore two-dimensional fiber consisting of 11×11 cores with length $500z_{\text{dis}}$. For these parameters, the dispersion length is equal to 5.7 and the beat length between adjacent modes is equal to 12. The continuous numbering of the cores,

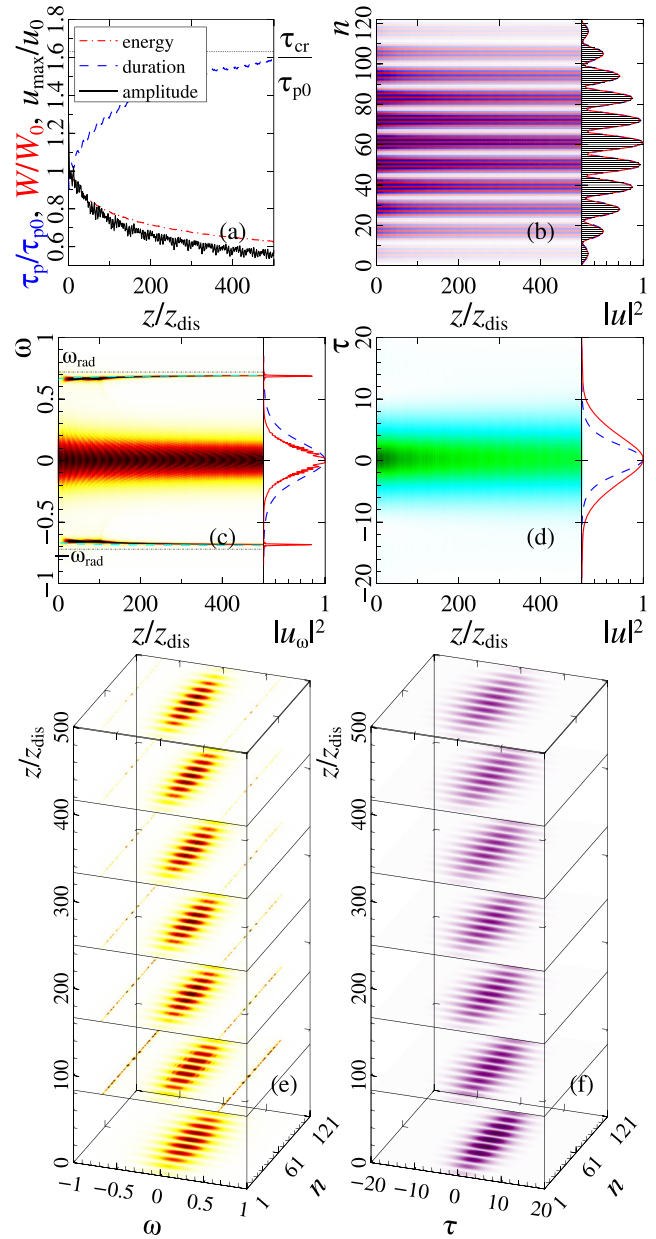


FIG. 8. Laser pulse dynamics in an MCF of 11×11 cores at $a = 2.2$. The continuous numbering of the cores, $k_{n,m} = n + Nm$, is used in the figure. Figure captions are similar to Fig. 2.

$k_{n,m} = n + Nm$, is used in the figure. The captions are similar to Fig. 2. It can be seen that a laser pulse propagating in an MCF radiates a dispersive wave at a frequency ω_{rad}^{2D} , which is different from the frequency in the case of a one-dimensional grating, ω_{rad}^{1D} . Below, an estimate of this frequency will be found. At the initial stage $z \lesssim 100z_{\text{dis}}$, the injected laser pulse intensively radiates a dispersive wave with an amplitude comparable to the one at $\omega = 0$. The width of the laser pulse spectrum decreases monotonically, and the duration, accordingly, increases as the energy in the wave packet decreases [Fig. 8(a)]. The laser pulse stops radiating when the dispersion length of the excited nonlinear structure exceeds the beat length between neighboring supermodes. Subsequently, the laser pulse propagates unchanged.

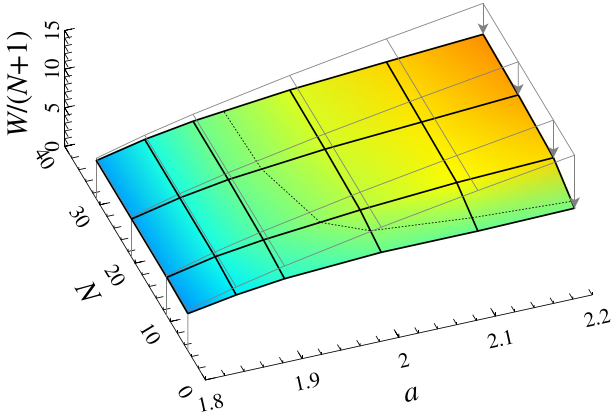


FIG. 9. Dependence of the final normalized energy W/N of the excited out-of-phase soliton in an MCF of $N \times N$ cores on the number N and the power parameter a . The dots show the critical energy level (36).

The stability analysis (36) and the results of numerical simulation (Fig. 8), as in the case of a one-dimensional grating, demonstrate the impossibility of a noticeable transformation of the transverse distribution of the wave field from an inhomogeneous profile to a uniform one with an increase in the parameter a . Figure 9 shows the final energy of an excited out-of-phase soliton in a two-dimensional lattice $N \times N$ as a function of the parameters N and a . The figure shows that this energy is proportional to the number of cores, N , in one of the directions, which is in good agreement with the above theoretical analysis (36). This is significantly different from a one-dimensional lattice of weakly coupled cores since the maximum achievable transported energy increases despite the limitation of the minimum duration of solitons. As in the case of a one-dimensional lattice, the growth of the soliton energy is limited with increasing parameter a due to the generation of a dispersive wave at the frequency $\omega_{\text{rad}}^{2\text{D}}$.

Let us obtain the frequency estimate $\omega_{\text{rad}}^{2\text{D}}$, proceeding in a similar way as was done in the case of a one-dimensional lattice. We will look for a solution of Eq. (4) in the form

$$u_{n,m} = (-1)^{n+m} \sin\left(\frac{\pi n}{N+1}\right) \sin\left(\frac{\pi m}{N+1}\right) A(z, \tau). \quad (38)$$

Substituting into the action of Eq. (4) for $M = N$, we find the truncated action,

$$S = \frac{(N+1)^2}{4} \iint \left[\frac{i}{2} \left(A \frac{\partial A^*}{\partial z} - A^* \frac{\partial A}{\partial z} \right) + 4 \cos\left(\frac{\pi}{N+1}\right) |A|^2 + \alpha \left| \frac{\partial A}{\partial \tau} \right|^2 - \frac{9}{32} |A|^4 \right]. \quad (39)$$

Its variation gives the NSE equation

$$i \frac{\partial A}{\partial z} + \alpha \frac{\partial^2 A}{\partial \tau^2} + \frac{9}{16} |A|^2 A - 4 \cos\left(\frac{\pi}{N+1}\right) A = 0, \quad (40)$$

whose soliton solution is

$$u_{n,m} = (-1)^{n+m} \frac{4 \sqrt{2\alpha/\tau_p}}{3 \cosh(\tau/\tau_p)} \times \sin\left(\frac{\pi n}{N+1}\right) \sin\left(\frac{\pi m}{N+1}\right) e^{-ik_{\text{sol}}^{2\text{D}} z}, \quad (41)$$

where $k_{\text{sol}}^{2\text{D}} = 2 \cos(\frac{\pi}{N+1}) - 9/32 u_0^2$ is the wave number of a soliton in a square lattice of weakly coupled cores, and u_0 is the amplitude of the soliton. The similar value of wave number $k_{\text{sol}}^{1\text{D}} \equiv -d\varphi/dz$ is obtained by varying the action [Eq. (33)] on W . Note that the energy of this solution is $W = \frac{32}{9} (N+1)^2 \alpha / \tau_p$; compare with Eq. (35). The linear dispersion relation of Eq. (4) for $u_{n,m} \propto (-1)^{n+m} e^{-ikz + i\kappa_n n + i\kappa_m m - i\omega\tau}$ has the form

$$k_{\text{dis}}^{2\text{D}} = \alpha \omega^2 + 2(\cos \kappa_n + \cos \kappa_m), \quad \kappa_n = \frac{\pi n}{N+1}. \quad (42)$$

It is obvious that the radiation threshold of a dispersive wave is lower in the case when the indices n, m do not change simultaneously. Due to the symmetry of the problem, the considered soliton can radiate a dispersive wave at the frequency ω_{rad} with odd n and m . Then the nearest radiation frequencies will correspond to $n = N, m = N - 2$ or $n = N - 2, m = N$ and give

$$\omega_{\text{rad}}^{2\text{D}} = \pm \frac{1}{\sqrt{\alpha}} \sqrt{4 \sin\left(\frac{\pi}{N+1}\right) \sin\left(\frac{2\pi}{N+1}\right) - \frac{9}{32} u_0^2}. \quad (43)$$

Let us return to the results of the numerical simulation. Cyan dashes in Fig. 8(c) show the found estimate [Eq. (43)] of the dispersive wave frequency, which is in good agreement with the numerical results. As the soliton amplitude decreases due to losses, the frequency of the dispersive wave shifts to the frequency determined in the limit of small amplitudes ($u_0 \approx 0$), which is shown in the figure by the black dash-dotted line.

V. CONCLUSION

The approximate solitonlike out-of-phase solutions for the wave field in an MCF with core configurations in the form of line $1 \times N$ and a square matrix $N \times N$ are found in the framework of the discrete nonlinear Schrödinger equation. The stability conditions for Eqs. (24) and (36) of the found solutions are determined, and the presence of the minimum duration τ_{cr} for their stability is shown. Numerical simulation confirms the stability of such solutions at durations $\tau_p \gtrsim \tau_{\text{cr}}$ and shows that the radiation of linear dispersive waves for shorter pulses rather quickly leads them to the found distribution with $\tau_p \sim \tau_{\text{cr}}$.

Thus, the maximum achievable energy of relatively long pulses, $\tau_p > \tau_{\text{cr}}$, grows in proportion to the number of cores. For example, the total energy of the out-of-phase distribution in a square MCF of $N \times N$ cores is about $N^2/2$ times higher than the energy of a NSE soliton of the same duration. However, the presence of the minimal duration $\tau_{\text{cr}} \propto N$ means that the maximum achievable transferred energy grows as little as N for a square matrix $N \times N$ of cores and does not

depend on the number of cores in a one-dimensional lattice. This makes such fibers less preferable for operating with extremely short solitons in comparison with MCFs with the ring configuration of cores [25]. However, the technological difficulties in manufacturing MCFs from a large number of cores equally distributed over the ring level out the limitations of out-of-phase distributions in MCFs with a square matrix of cores.

ACKNOWLEDGMENTS

This work was supported by the Russian Science Foundation Grant No. 23-12-00248, [26] regarding square lattices and by the Center of Excellence “Center of Photonics” funded by the Ministry of Science and Higher Education of the Russian Federation, Contract No. 075-15-2022-316 regarding one-dimensional lattices.

-
- [1] G. P. Agrawal, *Nonlinear Fiber Optics*, 6th ed. (Academic Press/Elsevier, Cambridge, 2019).
 - [2] I. Babushkin, A. Husakou, J. Herrmann, and Y. S. Kivshar, *Opt. Express* **15**, 11978 (2007).
 - [3] X. Qi, S. Chen, Z. Li, T. Liu, Y. Ou, N. Wang, and J. Hou, *Opt. Lett.* **43**, 1019 (2018).
 - [4] T. X. Tran, D. C. Duong, and F. Biancalana, *Phys. Rev. A* **89**, 013826 (2014).
 - [5] T. X. Tran, D. C. Duong, and F. Biancalana, *Phys. Rev. A* **90**, 023857 (2014).
 - [6] A. B. Aceves, G. G. Luther, C. De Angelis, A. M. Rubenchik, and S. K. Turitsyn, *Phys. Rev. Lett.* **75**, 73 (1995).
 - [7] A. A. Balakin, A. G. Litvak, and S. A. Skobelev, *Phys. Rev. A* **100**, 053830 (2019).
 - [8] A. B. Aceves, O. V. Shtyrina, A. M. Rubenchik, M. P. Fedoruk, and S. K. Turitsyn, *Phys. Rev. A* **91**, 033810 (2015).
 - [9] D. Cheskis, S. Bar-Ad, R. Morandotti, J. S. Aitchison, H. S. Eisenberg, Y. Silberberg, and D. Ross, *Phys. Rev. Lett.* **91**, 223901 (2003).
 - [10] A. Rubenchik, I. Chekhovskoy, M. Fedoruk, O. Shtyrina, and S. K. Turitsyn, *Opt. Lett.* **40**, 721 (2015).
 - [11] H. Leblond, D. Kremer, and D. Mihalache, *Phys. Rev. A* **95**, 043839 (2017).
 - [12] S. Minardi, F. Eilenberger, Y. V. Kartashov, A. Szameit, U. Ropke, J. Kobelke, K. Schuster, H. Bartelt, S. Nolte, L. Torner, F. Lederer, A. Tunnermann, and T. Pertsch, *Phys. Rev. Lett.* **105**, 263901 (2010).
 - [13] A. V. Andrianov, N. A. Kalinin, M. Y. Koptev, O. N. Egorova, A. V. Kim, and A. G. Litvak, *Opt. Lett.* **44**, 303 (2019).
 - [14] A. M. Rubenchik, E. V. Tkachenko, M. P. Fedoruk, and S. K. Turitsyn, *Opt. Lett.* **38**, 4232 (2013).
 - [15] A. A. Balakin, A. G. Litvak, V. A. Mironov, and S. A. Skobelev, *Phys. Rev. A* **94**, 063806 (2016).
 - [16] A. A. Balakin, S. A. Skobelev, E. A. Anashkina, A. V. Andrianov, and A. G. Litvak, *Phys. Rev. A* **98**, 043857 (2018).
 - [17] H. Tünnemann and A. Shirakawa, *Opt. Express* **23**, 2436 (2015).
 - [18] A. A. Balakin, S. A. Skobelev, and A. G. Litvak, *Europhys. Lett.* **132**, 54001 (2020).
 - [19] A. A. Balakin, S. A. Skobelev, A. V. Andrianov, E. A. Anashkina, and A. G. Litvak, *Opt. Lett.* **46**, 246 (2021).
 - [20] A. A. Balakin, A. G. Litvak, and S. A. Skobelev, *Phys. Rev. A* **100**, 053834 (2019).
 - [21] A. A. Balakin, S. A. Skobelev, A. V. Andrianov, E. A. Anashkina, and A. G. Litvak, *Opt. Lett.* **45**, 3224 (2020).
 - [22] D. N. Christodoulides and R. I. Joseph, *Opt. Lett.* **13**, 794 (1988).
 - [23] D. Anderson, M. Desaix, M. Karlsson, M. Lisak, and M. L. Quiroga-Teixeiro, *J. Opt. Soc. Am. B* **10**, 1185 (1993).
 - [24] <http://wxmaxima.sourceforge.net/>.
 - [25] S. A. Skobelev, A. A. Balakin, E. A. Anashkina, A. V. Andrianov, and A. G. Litvak, *Phys. Rev. A* **104**, 023522 (2021).
 - [26] <https://rscf.ru/en/project/23-12-00248/>.